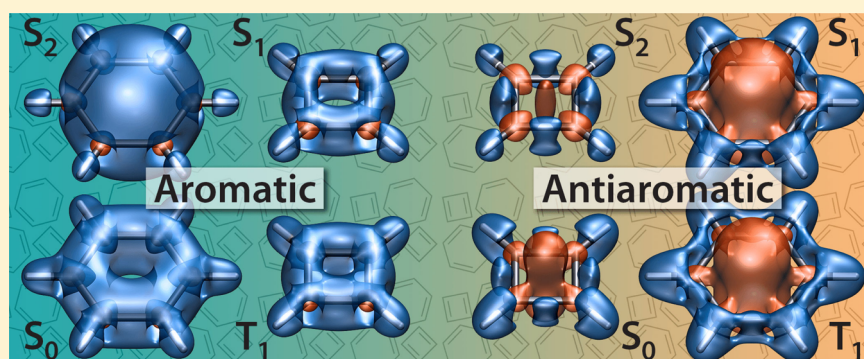


Magnetic Shielding, Aromaticity, Antiaromaticity, and Bonding in the Low-Lying Electronic States of Benzene and Cyclobutadiene

Peter B. Karadakov,* Peter Hearnshaw, and Kate E. Horner

Department of Chemistry, University of York, Heslington, York YO10 5DD, U.K.

S Supporting Information



ABSTRACT: Aromaticity, antiaromaticity, and their effects on chemical bonding in the ground states (S_0), lowest triplet states (T_1), and the first and second singlet excited states (S_1 and S_2) of benzene (C_6H_6) and square cyclobutadiene (C_4H_4) are investigated by analyzing the variations in isotropic magnetic shielding around these molecules in each electronic state. All shieldings are calculated using state-optimized π -space complete-active-space self-consistent field (CASSCF) wave functions constructed from gauge-including atomic orbitals (GIAOs), in the 6-311++G(2d,2p) basis. It is shown that the profoundly different shielding distributions in the S_0 states of C_6H_6 and C_4H_4 represent aromaticity and antiaromaticity “fingerprints” which are reproduced in other electronic states of the two molecules and allow classification of these states as aromatic (S_0 and S_2 for C_6H_6 , T_1 and S_1 for C_4H_4) or antiaromatic (S_0 and S_2 for C_4H_4 , T_1 and S_1 for C_6H_6). S_2 C_6H_6 is predicted to be even more aromatic than S_0 C_6H_6 . As isotropic shielding isosurfaces and contour plots show very clearly the effects of aromaticity and antiaromaticity on chemical bonding, these can be viewed, arguably, as the most succinct visual definitions of the two phenomena currently available.

1. INTRODUCTION

Whereas, up until recently, excited state aromaticity and antiaromaticity were regarded mainly as theoretical hypotheses (for an overview of the area, see the comprehensive review by Kilså, Ottosson et al.¹), now there are convincing experimental proofs, furnished by Kim, Osuka and co-workers, of aromaticity reversals in the lowest triplet states of bis-rhodium hexaphyrins,² and in the lowest singlet states of 1,3-phenylene-strapped [26]- and [28]hexaphyrins.³ The first of these targets is the better-known excited state aromaticity associated with Baird’s rule,⁴ according to which the familiar $4n + 2$ and $4n$ rules for ground-state aromaticity in cyclic conjugated hydrocarbons are switched over in their lowest triplet states: rings with $4n$ π electrons come out as aromatic while those with $4n + 2$ π electrons end up as antiaromatic; the second one addresses an analogous effect expected in the respective lowest singlet excited states.^{5,6} The increased interest in excited state aromaticity and antiaromaticity^{1,7} is creating demand for theoretical tools that are capable of providing detailed accounts of these phenomena and their implications for the properties of the excited states; such tools can aid the design of organic compounds with potential applications in organic electronics

and photovoltaics.¹ In this paper we show that these purposes are served very well by analyses of the off-nucleus isotropic magnetic shielding isosurfaces and contour plots for excited states.

The behavior of magnetic shielding tensors, $\sigma(\mathbf{r})$, calculated at various positions \mathbf{r} within the space surrounding a molecule carries a wealth of information about chemical bonding and, for cyclic conjugated systems, about aromaticity. Off-nucleus isotropic magnetic shieldings, $\sigma_{\text{iso}}(\mathbf{r}) = 1/3[\sigma_{xx}(\mathbf{r}) + \sigma_{yy}(\mathbf{r}) + \sigma_{zz}(\mathbf{r})]$, and out-of-plane components of $\sigma(\mathbf{r})$, $\sigma_{zz}(\mathbf{r})$, are involved in the definitions of nucleus-independent chemical shifts (NICS), popular single-point aromaticity indices introduced by Schleyer and co-workers. The original NICS index, NICS(0),⁸ was defined as $-\sigma_{\text{iso}}(\text{at ring center})$; subsequent attempts to improve the accuracy of relative aromaticity predictions led to the formulation of further NICS indices including NICS(1) = $-\sigma_{\text{iso}}(\text{at } 1 \text{ \AA above ring center})$,^{9,10} NICS(0)_{zz} = $-\sigma_{zz}(\text{at ring center})$,^{11,12} NICS(1)_{zz} =

Received: October 9, 2016

Published: October 27, 2016

$-\sigma_{zz}$ (at 1 Å above ring center),¹³ and various “dissected” NICS indices (for details, see e.g. ref 13).

An essential feature of NICS(0), NICS(1), NICS(0)_{zz}, and NICS(1)_{zz} is that these indices can be calculated not only by using the Hartree–Fock (HF) method and density functional theory (DFT) but also by means of post-HF methods accounting for electron correlation effects such as MP2 (second order Møller–Plesset perturbation theory) and CASSCF (complete-active-space self-consistent field). NICS(0), NICS(1), NICS(0)_{zz}, and NICS(1)_{zz} values obtained using CASSCF wave functions constructed from gauge-including atomic orbitals (GIAOs) were among the magnetic criteria used in the first post-HF ab initio assessments of the aromaticities of the low-lying electronic states of benzene, cyclobutadiene, and cyclooctatetraene.^{5,6} According to the results reported in refs 5, 6, these molecules which, in their electronic ground states (S_0), are regarded as classical examples of aromatic and antiaromatic systems exhibit complete changeovers of aromatic character in their lowest triplet states (T_1) and first singlet excited states (S_1): Benzene (D_{6h} symmetry) switches from aromatic in S_0 to antiaromatic in T_1 and S_1 , whereas cyclobutadiene and cyclooctatetraene in their highest-symmetry geometries (D_{4h} and D_{8h} respectively) switch from antiaromatic in S_0 to aromatic in T_1 and S_1 . The aromaticity reversals between different electronic states of benzene, cyclobutadiene, and cyclooctatetraene have been confirmed by Feixas, Solà et al.¹⁴ through an alternative approach that does not utilize magnetic properties, but involves the examination of electronic delocalization indices calculated using CASSCF wave functions.

A more versatile approach which goes beyond the single-point NICS idea is to examine how isotropic shielding varies within the space surrounding the molecular framework.^{15–22} Detailed $\sigma_{\text{iso}}(\mathbf{r})$ isosurfaces and contour plots constructed from dense regular grids of $\sigma_{\text{iso}}(\mathbf{r})$ values (as established in refs 19–22, a reasonable compromise between level of detail and computational effort is achieved by using a spacing of 0.05 Å) allow very clear distinction between aromaticity and antiaromaticity in the electronic ground states of benzene and cyclobutadiene and reveal how pronounced differences in aromatic character are reflected in chemical bonding.¹⁹ These isosurfaces and contour plots also help differentiate between the aromaticities of heterocycles with one and two heteroatoms^{20,21} and provide an easy-to-interpret picture of chemical bonding in hydrocarbons, which is more detailed than the traditional description in terms of the total electronic density.²² The analysis of the off-nucleus magnetic isotropic shielding as a function of position addresses some of the more important criticisms toward various types of single-point NICS, including the certain degree of arbitrariness in the choice of the positions at which single-point NICS are calculated and the fact that a single number might not be able to carry the information content required to characterize the aromaticity of a system; for example, it has been shown that different ring current maps can produce nearly indistinguishable single-point NICS values.^{23,24}

In this paper we use off-nucleus isotropic magnetic shielding isosurfaces and contour plots to study aromaticity, antiaromaticity, and chemical bonding in the low-lying electronic states of benzene and square cyclobutadiene. The electronic states examined, for both molecules, are S_0 , T_1 , S_1 , and S_2 , a selection similar to that from ref 5, with the addition of the second singlet excited state (S_2) of benzene. Following past

experience with evaluating magnetic properties of benzene and cyclobutadiene,^{5,19} in order to treat the different electronic states of the two molecules at a level of theory producing comparable qualitatively correct results, all calculations are carried out using state-optimized π -space CASSCF-GIAO wave functions. Previous research¹⁹ revealed profound differences between the isotropic shielding distributions in the ground electronic states of benzene and square cyclobutadiene: All carbon–carbon bonds in benzene were found to be enclosed within a doughnut-shaped region of increased shielding, indicative of strong bonding interactions, whereas square cyclobutadiene was shown to have a strongly deshielded dumbbell-shaped region in the center of the molecule, causing partial disruption of the carbon–carbon bonds and antiaromatic destabilization. Our main aim is to establish whether similar differences are also observed in the low-lying electronic excited states of these molecules which would provide strong support, from an approach free from the shortcomings of single-point NICS indices, for the conclusions about aromaticity and antiaromaticity in the T_1 and S_1 states made in ref 5, help decide on the aromaticities of the S_2 states, and prove that analyses of the off-nucleus isotropic magnetic shielding isosurfaces and contour plots can be used to obtain detailed information about aromaticity, antiaromaticity, and bonding in the excited states of key organic compounds.

2. COMPUTATIONAL PROCEDURE

All CASSCF-GIAO calculations on benzene and cyclobutadiene reported in this paper were carried out using the MCSCF-GIAO (multiconfigurational SCF with GIAOs) methodology introduced in refs 25, 26 and implemented in the Dalton 2016.0 program package,²⁷ within the 6-311++G(2d,2p) basis.

The S_0 (1^1A_{1g}), T_1 (1^3B_{1u}), S_1 (1^1B_{2u}), and S_2 (1^1B_{1u}) electronic states of benzene were described using state-optimized π -space CASSCF(6,6) wave functions (with “6 electrons in 6 orbitals”), at the experimental D_{6h} gas-phase ground-state geometry with C–C and C–H bond lengths of 1.3964 and 1.0831 Å, respectively, established through analysis of the ν_4 vibration–rotation bands of C_6H_6 and C_6D_6 .²⁸

The calculations on the S_0 (1^1B_{1g}), T_1 (1^3A_{2g}), S_1 (1^1A_{1g}), and S_2 (1^1B_{2g}) electronic states of square cyclobutadiene employed state-optimized π -space CASSCF(4,4) wave functions (with “4 electrons in 4 orbitals”), at the D_{4h} geometry with C–C and C–H bond lengths of 1.447 and 1.076 Å, respectively, optimized through a multireference averaged quadratic coupled cluster (MR-AQCC) approach with orbitals taken from state-averaged π -space CASSCF(4,4) wave functions including the ground state, lowest triplet state, and two lowest singlet excited states (SA-4-CASSCF), within the cc-pVTZ basis.²⁹

The geometries of benzene and square cyclobutadiene chosen for the current calculations are identical to those used in refs 5, 19.

As a result of the decision to use ground-state geometries for all excited states, the comparisons between the properties of the electronic states of benzene and cyclobutadiene are in the context of vertical excitations. While the lowest energy geometries of aromatic electronic states can be expected to remain reasonably similar to the D_{6h} and D_{4h} geometries of benzene and cyclobutadiene, respectively, used in the calculations, the lowest-energy geometries of electronic states classified as antiaromatic are likely to exhibit significantly lower

Table 1. Carbon and Proton Isotropic Shieldings, and NICS(0), NICS(1), NICS(0)_{zz} and NICS(1)_{zz} Values for the S₀, T₁, S₁, and S₂ Electronic States of Benzene and Square Cyclobutadiene (in ppm)^a

molecule	state	$\sigma_{\text{iso}}(^{13}\text{C})$	$\sigma_{\text{iso}}(^1\text{H})$	NICS(0)	NICS(1)	NICS(0) _{zz}	NICS(1) _{zz}
C ₆ H ₆	S ₀ (1 ¹ A _{1g})	73.52	24.90	-8.17	-9.53	-12.21	-27.83
	T ₁ (1 ³ B _{1u})	81.89	29.31	39.63	30.10	130.54	90.61
	S ₁ (1 ¹ B _{2u})	78.69	29.54	45.81	34.67	145.90	102.76
	S ₂ (1 ¹ B _{1u})	75.42	21.25	-39.08	-36.68	-119.47	-117.59
C ₄ H ₄	S ₀ (1 ¹ B _{1g})	68.24	27.60	36.41	28.23	145.91	88.14
	T ₁ (1 ³ A _{2g})	71.75	25.15	-3.74	-6.54	24.26	-16.47
	S ₁ (1 ¹ A _{1g})	54.80	23.96	3.44	-4.28	24.61	-16.38
	S ₂ (1 ¹ B _{2g})	15.85	22.88	22.10	12.86	77.09	31.24

^aFor further details, see text.

symmetries, due to distortions that reduce the antiaromatic character, such as the well-known D_{4h} to D_{2h} (“square” to “rectangle”) symmetry reduction in the electronic ground state of cyclobutadiene.

Following previous work on NICS^{5,6,30} and ring currents³¹ in triplet systems, the CASSCF-GIAO isotropic shieldings in the T₁ states of benzene and cyclobutadiene reported in this paper include the contributions arising from the perturbation to the wave function only (often referred to as “orbital” contributions in single-determinant approaches). While this choice is convenient for the purposes of the current study, as the values reported for a triplet state become directly comparable to those for singlet states, a more rigorous treatment would need to take into account the large terms associated with the interaction between the electronic spin angular momentum and the magnetic field.^{32,33}

The grids of points used in the construction of $\sigma_{\text{iso}}(\mathbf{r})$ isosurfaces and contour plots for the S₀, T₁, S₁, and S₂ electronic states of benzene and cyclobutadiene were defined similarly to the grids employed for the S₀ electronic states of these molecules in ref 19: The grid for each molecule is regular, with a spacing of 0.05 Å, includes 141³ points (C₆H₆) or 101³ points (C₄H₄), and takes the shape of a cube with edges of 7 Å (C₆H₆) or 5 Å (C₄H₄), centered at the origin of a center-of-mass right-handed Cartesian coordinate system in which the z axis is perpendicular to the molecular plane and the x axis passes through the midpoints of two carbon–carbon bonds. In order to reduce computational effort, for each electronic state $\sigma_{\text{iso}}(\mathbf{r})$ values were calculated only at the 71³ points (C₆H₆) or 51³ points (C₄H₄) within one octant of the respective grid and replicated by symmetry. For visualization purposes, all $\sigma_{\text{iso}}(\mathbf{r})$ values obtained for the various electronic states of C₆H₆ and C₄H₄ were assembled in GAUSSIAN cube files.³⁴

3. RESULTS AND DISCUSSION

The energies of the CASSCF(6,6)/6-311++G(2d,2p) wave functions for the S₀, T₁, and S₁ states of benzene and the CASSCF(4,4)/6-311++G(2d,2p) wave functions for the S₀, T₁, S₁, and S₂ states of square cyclobutadiene computed in this paper turned out to be exactly the same as those reported in ref 5. As it was noted in ref 5, the CASSCF(6,6)/6-311++G(2d,2p) S₀ to T₁ and S₀ to S₁ vertical excitation energies for benzene agree very well with experimental data^{35,36} and higher-level theoretical estimates;³⁷ in square cyclobutadiene, the CASSCF(4,4)/6-311++G(2d,2p) S₀ to T₁, S₀ to S₁, and S₀ to S₂ vertical excitation energies show some improvement over CASSCF(4,4)/6-31G results³⁸ but, due to the limited sizes of the singlet and triplet “4 in 4” active spaces, remain somewhat

higher than the values obtained using more advanced theoretical methods.²⁹

The CASSCF(6,6)/6-311++G(2d,2p) calculation for the S₂ electronic state of benzene produced an energy of -230.550 895 au which corresponds to an S₀ to S₂ vertical excitation energy of 7.82 eV. This vertical excitation energy is higher than the experimental value of 6.20 eV,³⁶ but in line with other theoretical results coming from π -space wave functions; for example, the result of a CASSCF(6,6) calculation in an ANO basis was almost the same, 7.85 eV,³⁹ and a much larger spin-coupled valence bond (SCVB) wave function yielded 7.49 eV.³⁷ In this case, achieving better agreement with experiment requires inclusion of dynamic correlation between the electrons in σ and π orbitals: Second-order perturbation theory with a CASSCF(6,12) π -space reference (CASPT2) gave an S₀ to S₂ vertical excitation energy of 6.10 eV.³⁹

The carbon and proton isotropic shieldings, and the NICS(0), NICS(1), NICS(0)_{zz}, and NICS(1)_{zz} values for the S₀, T₁, S₁, and S₂ electronic states of benzene and square cyclobutadiene, extracted from the current calculations of shielding tensors at the respective grids of points, are shown in Table 1. The numbers for states other than the S₂ electronic state of benzene are identical to those reported in ref 5 and have been included in order to facilitate comparison with the rather unexpected magnetic features of this state. The NICS(0), NICS(1), NICS(0)_{zz}, and NICS(1)_{zz} values for the S₂ electronic state of benzene indicate that in this state benzene becomes highly aromatic, significantly more so than in its ground electronic state (S₀). This conclusion is reinforced by the observation that S₂ benzene exhibits significant proton deshielding; the corresponding $\sigma_{\text{iso}}(^1\text{H})$ value is 3.65 ppm lower than its S₀ counterpart.

Interestingly, the findings of Feixas, Solà et al.¹⁴ about the S₂ electronic state of benzene are rather different. According to these authors, the S₂ and S₃ electronic states of benzene are degenerate; some electronic delocalization indices show that these states exhibit lower aromaticity than S₀, whereas other electronic delocalization indices suggest that S₂ and S₃ are either more antiaromatic or less antiaromatic than S₁. In fact, the S₂ (1 ¹B_{1u}) electronic state of benzene is well-known to be nondegenerate (see, e.g., refs 37, 39). The reported degeneracy of S₂ and S₃ and identical S₀ to S₂ and S₀ to S₃ vertical excitation energies of 8.17 eV indicate that the authors of ref 14 were not looking at S₂ and S₃, but at the two components of the degenerate S₄ (1 ¹E_{2g}). The order of the benzene S₃ (1 ¹E_{1u}) and S₄ (1 ¹E_{2g}) electronic states is reversed in π -space CASSCF(6,6) calculations; the corresponding vertical excitation energies obtained in an ANO basis are 9.29 eV (S₀ to S₃)

and 8.11 eV (S_0 to S_4), respectively.³⁹ Getting the S_3 and S_4 states in the correct order requires inclusion of dynamic correlation between the electrons in σ and π orbitals, for example, through CASPT2.³⁹

The ^{13}C isotropic shieldings in benzene increase by 5.17 ppm on passing from S_0 to S_1 , but then decrease by 3.27 ppm between S_1 and S_2 . These differences are much smaller in magnitude than the substantial decreases of the ^{13}C isotropic shieldings in the S_0 , S_1 , S_2 sequence of electronic states in square cyclobutadiene. Thus, while it can be expected that, in general, electronic excitation would be accompanied by nuclear deshielding, especially for heavier nuclei,⁵ some low-lying electronic states may show exceptions.

The spatial variations in isotropic shielding, $\sigma_{\text{iso}}(\mathbf{r})$, for the S_0 , T_1 , S_1 , and S_2 states of benzene and square cyclobutadiene are illustrated in Figures 1–6. The isotropic shielding isosurfaces

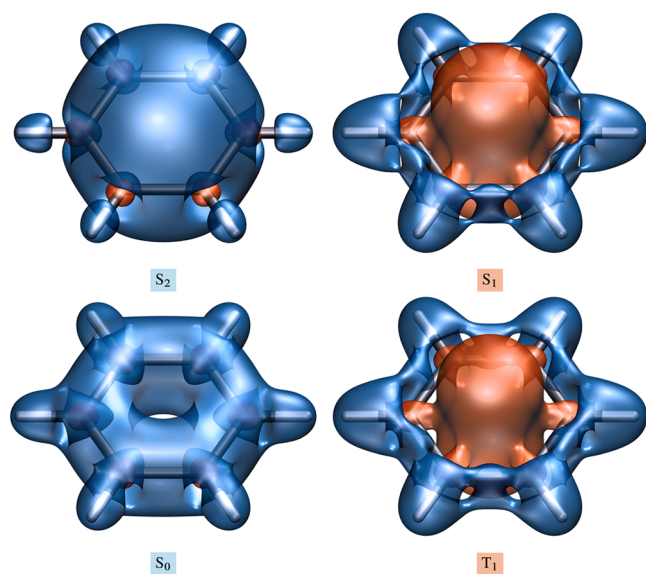


Figure 1. Isotropic shielding isosurfaces at $\sigma_{\text{iso}}(\mathbf{r}) = \pm 16$ ppm for the S_0 , T_1 , S_1 , and S_2 states of benzene obtained using state-optimized π -space CASSCF(6,6)-GIAO/6-311++G(2d,2p) wave functions (positive isovalue in blue).

and contour plots for the ground electronic states (S_0) of both molecules are very similar to the respective isosurfaces and contour plots obtained previously using CASSCF(6,6)-GIAO and CASSCF(4,4)-GIAO wave functions in the smaller 6-311++G(d,p) basis.¹⁹ While the current S_0 isotropic shielding isosurfaces calculated in the 6-311++G(2d,2p) basis (see Figures 1 and 2) are visually indistinguishable from the corresponding 6-311++G(d,p) isosurfaces,¹⁹ the more detailed S_0 $\sigma_{\text{iso}}(\mathbf{r})$ contour plots (see Figures 3–6) indicate that the use of a larger basis leads to some deshielding in regions close to the ring centers.

The shapes of the isotropic shielding isosurfaces and contour plots in Figures 1–6 show clearly that the profoundly different isotropic shielding distributions in the electronic ground states of benzene and square cyclobutadiene, reported initially in ref 19 and confirmed in the current work, can be viewed as aromaticity and antiaromaticity “fingerprints” which are closely reproduced in other low-lying electronic states of the two molecules and allow the unambiguous classification of these states as aromatic or antiaromatic.

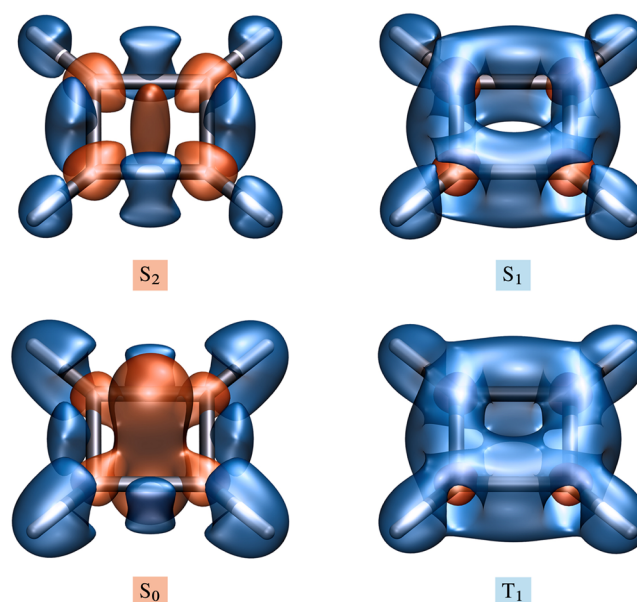


Figure 2. Isotropic shielding isosurfaces at $\sigma_{\text{iso}}(\mathbf{r}) = \pm 16$ ppm for the S_0 , T_1 , S_1 , and S_2 states of square cyclobutadiene obtained using state-optimized π -space CASSCF(4,4)-GIAO/6-311++G(2d,2p) wave functions (positive isovalue in blue).

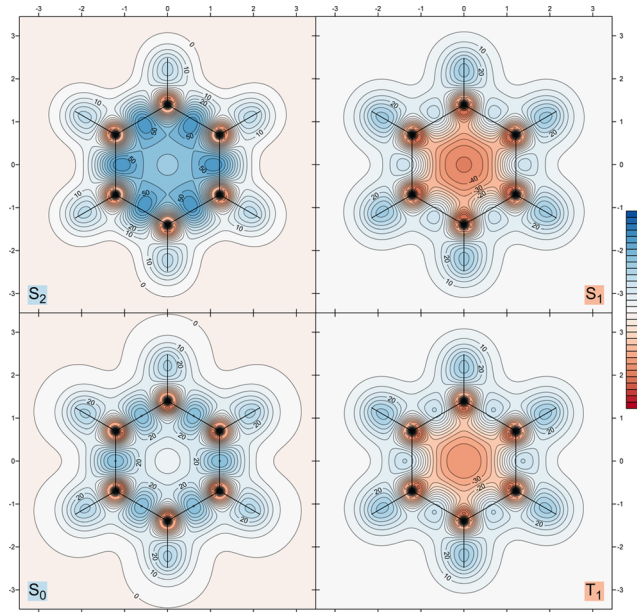


Figure 3. Isotropic shielding contour plots in the molecular (horizontal) plane for the S_0 , T_1 , S_1 , and S_2 states of benzene (wave functions as for Figure 1, $\sigma_{\text{iso}}(\mathbf{r})$ in ppm, axes in Å).

In the S_0 electronic state of benzene the carbon ring is enclosed within a doughnut-shaped region of increased shielding, inside which $\sigma_{\text{iso}}(\mathbf{r})$ reaches 45.07 ppm at the midpoint of each carbon–carbon bond. Similar pictures, suggesting strong bonding interactions and aromatic stability (although not up to S_0 benzene levels), are observed in the T_1 and S_1 electronic states of square cyclobutadiene. In both of these states the positions of maximal shielding near carbon–carbon bonds, corresponding to $\sigma_{\text{iso}}(\mathbf{r})$ values of 39.14 ppm for T_1 and 35.34 ppm for S_1 , are displaced toward the exterior of the ring (see Figure 4). In the S_2 electronic state of benzene the

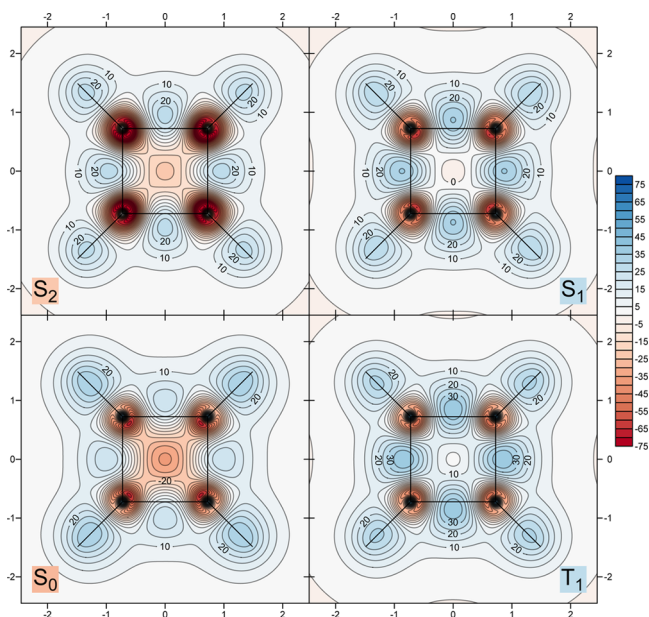


Figure 4. Isotropic shielding contour plots in the molecular (horizontal) plane for the S_0 , T_1 , S_1 , and S_2 states of square cyclobutadiene (wave functions as for Figure 2, $\sigma_{\text{iso}}(\mathbf{r})$ in ppm, axes in Å).

interior of the carbon ring is so intensely shielded that, in order to obtain a doughnut-shaped isotropic shielding isosurface, the $\sigma_{\text{iso}}(\mathbf{r})$ isovalue would need to exceed 40 ppm (see Figure 5). In this state, the maximal shieldings near carbon–carbon bonds reach 59.74 ppm, at positions displaced toward the interior of the ring (see Figure 3).

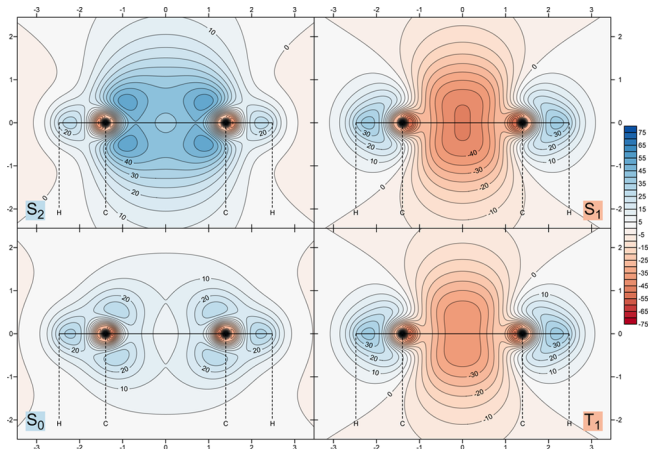


Figure 5. Isotropic shielding contour plots in the vertical plane passing through two carbons and two hydrogens for the S_0 , T_1 , S_1 , and S_2 states of benzene (wave functions as for Figure 1, $\sigma_{\text{iso}}(\mathbf{r})$ in ppm, axes in Å).

Antiaromatic destabilization in the S_0 electronic state of square cyclobutadiene can be attributed to the presence of a markedly deshielded dumbbell-shaped region in the center of the molecule which disrupts the linkages between the shielded regions corresponding to individual carbon–carbon bonds, reduces shielding within these regions, and displaces them to off-bond locations outside the ring. The maxima of 24.38 ppm achieved within shielded regions near carbon–carbon bonds are significantly lower than the corresponding values for

aromatic electronic states. Similar central deshielded regions affecting adversely bonding along the respective carbon frameworks appear, even more prominently, in the T_1 and S_1 electronic states of benzene and, less prominently, in the S_2 electronic state of square cyclobutadiene. In all three states the shielded regions near carbon–carbon bonds are mostly outside the rings; the shielding maxima observed within these regions are 25.33 ppm for T_1 C_6H_6 , 22.69 ppm for S_1 C_6H_6 , and 27.97 ppm for S_2 C_4H_4 .

The isotropic shielding isosurfaces and contour plots for the S_0 , T_1 , S_1 and S_2 states of benzene and square cyclobutadiene in Figures 1–6 clearly show that, in terms of relative aromaticity,

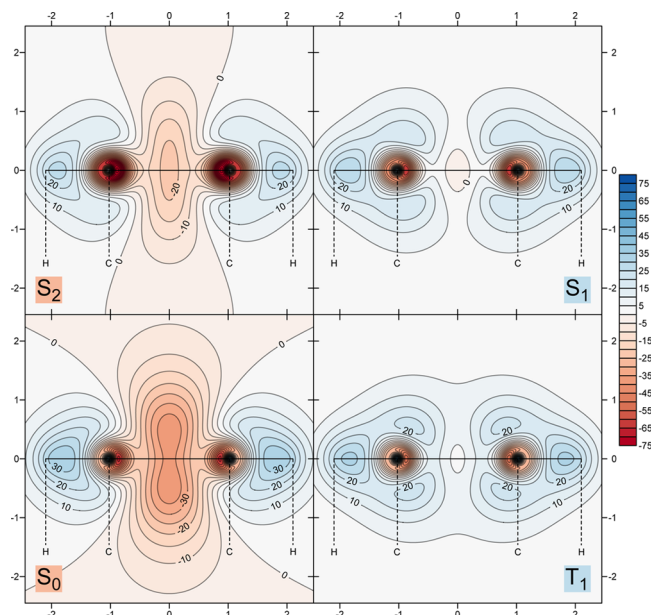


Figure 6. Isotropic shielding contour plots in the vertical plane passing through two carbons and two hydrogens for the S_0 , T_1 , S_1 , and S_2 states of square cyclobutadiene (wave functions as for Figure 2, $\sigma_{\text{iso}}(\mathbf{r})$ in ppm, axes in Å).

the eight electronic states studied in this paper are ordered from more aromatic to less aromatic (or more antiaromatic) as S_2 C_6H_6 > S_0 C_6H_6 > T_1 C_4H_4 > S_1 C_4H_4 > S_2 C_4H_4 > S_0 C_4H_4 > T_1 C_6H_6 > S_1 C_6H_6 .

As can be seen in Figures 1–6, the shielded regions enveloping carbon–hydrogen bonds in antiaromatic electronic states (S_0 C_4H_4 , T_1 C_6H_6 and S_1 C_6H_6) are, in general, larger and more intense than the corresponding regions in aromatic electronic states (S_0 C_6H_6 , S_2 C_6H_6 , T_1 C_4H_4 , and S_1 C_4H_4). The noticeable overall deshielding of the molecular surroundings in S_2 C_4H_4 makes this electronic state an exception to the rule. Further confirmation of these observations is provided by the shielding maxima achieved along carbon–hydrogen bonds in antiaromatic electronic states (34.62 ppm in S_0 C_4H_4 , 37.03 ppm in T_1 C_6H_6 , and 37.18 ppm in S_1 C_6H_6) which are higher than their counterparts in aromatic electronic states (31.36 ppm in S_0 C_6H_6 , 27.29 ppm in S_2 C_6H_6 , 31.52 ppm in T_1 C_4H_4 , and 29.57 ppm in S_1 C_4H_4); the corresponding value for S_2 C_4H_4 is 27.30 ppm.

In all eight electronic states of benzene and square cyclobutadiene studied in this paper, the carbon nuclei are surrounded by small, nearly spherical, shielded regions with radii under 0.07 Å inside each of which $\sigma_{\text{iso}}(\mathbf{r})$ rapidly falls from the respective $\sigma_{\text{iso}}(^{13}\text{C})$ value to zero (see the dark circles

around carbons in Figures 3–6). These small shielded regions are enclosed within larger ovoid deshielded regions, inside which the $\sigma_{\text{iso}}(\mathbf{r})$ values are negative. In an antiaromatic electronic state the ovoid deshielded regions around carbons merge with the larger deshielded region in the center of the molecule. Similar deshielded “halos” around sp^2 and sp hybridized carbons and other sp^2 hybridized second-row atoms have been observed previously, not only in conjugated rings^{19–21} but also in open-chain conjugated molecules such as ethene, ethyne, and *s-trans*-1,3-butadiene.²² This suggests that the deshielded “halos” are a sign of a specific type of π electron behavior, characteristic of some sp^2 and sp hybridized second-row atoms and different from traditional ring currents. In general, the lowest $\sigma_{\text{iso}}(\mathbf{r})$ values within the deshielded “halos” in the electronic states of square cyclobutadiene (–66.54 ppm in S_0 , –52.94 ppm in T_1 , –65.12 ppm in S_1 , and –102.42 ppm in S_2) are lower than their counterparts in benzene (–46.44 ppm in S_0 , –51.07 ppm in T_1 , –54.87 ppm in S_1 , and –40.39 ppm in S_2); in each molecule the “halos” are more deshielded in antiaromatic electronic states.

In principle, isotropic shielding isosurfaces and contour plots can be used to analyze chemical bonding and, for cyclic conjugated systems, aromaticity and antiaromaticity, in any electronic state that can be described reliably by a wave function for which one can compute off-nucleus magnetic shielding tensors. At present, the only way to target electronic states other than the ground state is to utilize the MCSCF-GIAO code in Dalton²⁷ which is capable of performing state-optimized CASSCF-GIAO calculations. This would create certain computational difficulties if an attempt were made to analyze the aromaticities of higher electronic states of benzene and square cyclobutadiene. Let us take benzene as an example. As it was already mentioned, the order of the S_3 and S_4 electronic states is reversed in π -space CASSCF(6,6) calculations. Getting these states in the correct order requires inclusion of dynamic correlation between the electrons in σ and π orbitals, which would also help with obtaining more accurate vertical excitation energies for S_2 and higher electronic states. Additionally, each of the S_3 (1^1E_{1u}) and S_4 (1^1E_{2g}) electronic states is doubly degenerate, and so is T_2 (1^3E_{1u}). The standard way of dealing with degenerate electronic states is to perform state-averaged CASSCF calculations. So, making progress with higher electronic states of benzene would require, as a minimum, an SA-CASSCF code with GIAOs; for more accurate results, one would also need a code capable of calculating magnetic shielding tensors with GIAOs using CASPT2 or another multireference perturbation theory approach.

4. CONCLUSIONS

The analysis of the spatial variations in isotropic shielding, $\sigma_{\text{iso}}(\mathbf{r})$, for the ground, lowest triplet, and first and second singlet excited electronic states of benzene and square cyclobutadiene demonstrates that the key features of one of the two profoundly different isotropic shielding distributions in the electronic ground states of these molecules, reported initially in ref 19 and confirmed in the current work, are reproduced, with a substantial degree of similarity, in each of the other low-lying electronic states that were investigated.

The doughnut-shaped region of increased shielding enclosing the carbon ring in the electronic ground state of benzene, which is indicative of strong bonding interactions and aromatic stability, is also observed in the lowest triplet and first singlet

electronic excited states of square cyclobutadiene. In the second singlet excited electronic state of benzene which, according to the results of this work, is even more aromatic than the ground state, the whole interior of the carbon ring is so intensely shielded that the $\sigma_{\text{iso}}(\mathbf{r}) = 16$ ppm isosurface we usually examine becomes nearly spherical in shape, with small indentations around the carbon atoms.

The main cause for antiaromatic destabilization in the ground electronic state of square cyclobutadiene, a sizable markedly deshielded region in the center of the molecule which disrupts the linkages between the shielded regions corresponding to individual carbon–carbon bonds and thus weakens these bonds, is also present, even more prominently, in the lowest triplet and first singlet electronic excited states of benzene. This antiaromatic feature is still obvious but less pronounced in the isotropic shielding distribution for the second singlet excited electronic state of square cyclobutadiene.

These observations indicate that the isotropic shielding distributions in the electronic ground states of benzene and square cyclobutadiene represent general aromaticity and antiaromaticity “fingerprints” that can be used to identify the aromatic character of an electronic state of a cyclic conjugated system.

Benzene starts as aromatic in its electronic ground state, becomes antiaromatic in the first singlet excited state, and then reverts to aromatic in the second singlet excited state. Square cyclobutadiene alternates between antiaromatic in the electronic ground state, aromatic in the first singlet excited state, and antiaromatic in the second singlet excited state. These sequences suggest an aromaticity rule for singlet excited electronic states, according to which Hückel-aromatic rings with $4n + 2$ π electrons become antiaromatic in the first singlet excited state and switch back to aromatic in the second singlet excited state, whereas Hückel-antiaromatic rings with $4n$ π electrons become aromatic in the first singlet excited state and revert to antiaromatic in the second singlet excited state.

The most important advantage of the analysis of the spatial variations in isotropic shielding over single value aromaticity indices is that, in addition to providing information about relative aromaticity and antiaromaticity, the isotropic shielding isosurfaces and contour plots show very clearly the effects of aromaticity and antiaromaticity on chemical bonding which, arguably, can be viewed as the most succinct visual definitions of these phenomena currently available.

■ ASSOCIATED CONTENT

Supporting Information

The Supporting Information is available free of charge on the ACS Publications website at DOI: 10.1021/acs.joc.6b02460.

GAUSSIAN cube files containing all $\sigma_{\text{iso}}(\mathbf{r})$ values for the S_0 , T_1 , S_1 , and S_2 states of benzene and square cyclobutadiene obtained in the current paper (ZIP)

■ AUTHOR INFORMATION

Corresponding Author

*E-mail: peter.karadakov@york.ac.uk.

Notes

The authors declare no competing financial interest.

■ ACKNOWLEDGMENTS

The authors thank the Department of Chemistry of the University of York for a Teaching Scholarship to K.E.H.

REFERENCES

- (1) Rosenberg, M.; Dahlstrand, C.; KilsÅ, K.; Ottosson, H. *Chem. Rev.* **2014**, *114*, 5379–5425.
- (2) Sung, Y. M.; Yoon, M.-C.; Lim, J. M.; Rath, H.; Naoda, K.; Osuka, A.; Kim, D. *Nat. Chem.* **2015**, *7*, 418–422.
- (3) Sung, Y. M.; Oh, J.; Kim, W.; Mori, H.; Osuka, A.; Kim, D. *J. Am. Chem. Soc.* **2015**, *137*, 11856–11859.
- (4) Baird, N. C. *J. Am. Chem. Soc.* **1972**, *94*, 4941–4948.
- (5) Karadakov, P. B. *J. Phys. Chem. A* **2008**, *112*, 7303–7309.
- (6) Karadakov, P. B. *J. Phys. Chem. A* **2008**, *112*, 12707–12713.
- (7) Ottosson, H.; Borbas, K. E. *Nat. Chem.* **2015**, *7*, 373–375.
- (8) Schleyer, P. v. R.; Maerker, C.; Dransfeld, A.; Jiao, H.; Hommes, N. J. R. v. E. *J. Am. Chem. Soc.* **1996**, *118*, 6317–6318.
- (9) Schleyer, P. v. R.; Jiao, H.; Hommes, N. J. R. v. E.; Malkin, V. G.; Malkina, O. L. *J. Am. Chem. Soc.* **1997**, *119*, 12669–12670.
- (10) Schleyer, P. v. R.; Manoharan, M.; Wang, Z. X.; Kiran, B.; Jiao, H.; Puchta, R.; Hommes, N. J. R. v. E. *Org. Lett.* **2001**, *3*, 2465–2468.
- (11) Cernusak, I.; Fowler, P. W.; Steiner, E. *Mol. Phys.* **2000**, *98*, 945–953.
- (12) Steiner, E.; Fowler, P. W.; Jenneskens, L. W. *Angew. Chem., Int. Ed.* **2001**, *40*, 362–366.
- (13) Fallah-Bagher-Shaidaei, H.; Wannere, C. S.; Corminboeuf, C.; Puchta, R.; Schleyer, P. v. R. *Org. Lett.* **2006**, *8*, 863–866.
- (14) Feixas, F.; Vandenbussche, J.; Bultinck, P.; Matito, E.; Solà, M. *Phys. Chem. Chem. Phys.* **2011**, *13*, 20690–20703.
- (15) Klod, S.; Kleinpeter, E. *J. Chem. Soc., Perkin Trans. 2* **2001**, 1893–1898.
- (16) Kleinpeter, E.; Klod, S.; Koch, A. *J. Mol. Struct.: THEOCHEM* **2007**, *811*, 45–60.
- (17) Kleinpeter, E.; Koch, A. *Phys. Chem. Chem. Phys.* **2012**, *14*, 8742–8746.
- (18) Kleinpeter, E.; Koch, A. *J. Phys. Chem. A* **2012**, *116*, 5674–5680.
- (19) Karadakov, P. B.; Horner, K. E. *J. Phys. Chem. A* **2013**, *117*, 518–523.
- (20) Horner, K. E.; Karadakov, P. B. *J. Org. Chem.* **2013**, *78*, 8037–8043.
- (21) Horner, K. E.; Karadakov, P. B. *J. Org. Chem.* **2015**, *80*, 7150–7157.
- (22) Karadakov, P. B.; Horner, K. E. *J. Chem. Theory Comput.* **2016**, *12*, 558–563.
- (23) Fias, S.; Fowler, P. W.; Delgado, J. L.; Hahn, U.; Bultinck, P. *Chem. - Eur. J.* **2008**, *14*, 3093–3099.
- (24) Van Damme, S.; Acke, G.; Havenith, R. W. A.; Bultinck, P. *Phys. Chem. Chem. Phys.* **2016**, *18*, 11746–11755.
- (25) Ruud, K.; Helgaker, T.; Kobayashi, R.; Jørgensen, P.; Bak, K. L.; Jensen, H. J. A. *J. Chem. Phys.* **1994**, *100*, 8178–8185.
- (26) Ruud, K.; Helgaker, T.; Bak, K. L.; Jørgensen, P.; Olsen, J. *Chem. Phys.* **1995**, *195*, 157–169.
- (27) Aidas, K.; Angeli, C.; Bak, K. L.; Bakken, V.; Bast, R.; Boman, L.; Christiansen, O.; Cimiraglia, R.; Coriani, S.; Dahle, P.; Dalskov, E. K.; Ekström, U.; Enevoldsen, T.; Eriksen, J. J.; Ettenhuber, P.; Fernández, B.; Ferrighi, L.; Fliegl, H.; Frediani, L.; Hald, K.; Halkier, A.; Hättig, C.; Heiberg, H.; Helgaker, T.; Hennum, A. C.; Hettrema, H.; Hjertenæs, R.; Høst, S.; Høyvik, I.-M.; Iozzi, M. F.; Jansík, B.; Jensen, H. J. A.; Jonsson, D.; Jørgensen, P.; Kauczor, J.; Kirpekar, S.; Kjergaard, T.; Klopper, W.; Knecht, S.; Kobayashi, R.; Koch, H.; Kongsted, J.; Krapp, A.; Kristensen, K.; Ligabue, A.; Lutnæs, O. B.; Melo, J. I.; Mikkelsen, K. V.; Myhre, R. H.; Neiss, C.; Nielsen, C. B.; Norman, P.; Olsen, J.; Olsen, J. M. H.; Osted, A.; Packer, M. J.; Pawłowski, F.; Pedersen, T. B.; Provasi, P. F.; Reine, S.; Rinkevicius, Z.; Ruden, T. A.; Ruud, K.; Rybkin, V. V.; Salek, P.; Samson, C. C. M.; Sánchez de Merás, A.; Saue, T.; Sauer, S. P. A.; Schimmelpennig, B.; Sneskov, K.; Steindal, A. H.; Sylvester-Hvid, K. O.; Taylor, P. R.; Teale, A. M.; Tellgren, E. I.; Tew, D. P.; Thorvaldsen, A. J.; Thøgersen, L.; Vahtras, O.; Watson, M. A.; Wilson, D. J. D.; Ziolkowski, M.; Ågren, H. *WIREs Comput. Mol. Sci.* **2014**, *4*, 269–284. *Dalton, a Molecular Electronic Structure Program, Release Dalton2016.0*, 2015; see <http://daltonprogram.org>.
- (28) Cabana, A.; Bachand, J.; Giguère, J. *Can. J. Phys.* **1974**, *52*, 1949–1955.
- (29) Eckert-Maksić, M.; Vazdar, M.; Barbatti, M.; Lischka, H.; Maksić, Z. B. *J. Chem. Phys.* **2006**, *125*, 64310.
- (30) Gogonea, V.; Schleyer, P. v. R.; Schreiner, P. R. *Angew. Chem., Int. Ed.* **1998**, *37*, 1945–1948.
- (31) Fowler, P. W.; Steiner, E.; Jenneskens, L. W. *Chem. Phys. Lett.* **2003**, *371*, 719–723.
- (32) Rinkevicius, Z.; Vaara, J.; Telyatnyk, L.; Vahtras, O. *J. Chem. Phys.* **2003**, *118*, 2550–2561.
- (33) Vaara, J. *Phys. Chem. Chem. Phys.* **2007**, *9*, 5399–5418.
- (34) See http://www.gaussian.com/g_tech/g_ur/u_cubegen.htm.
- (35) Doering, J. P. *J. Chem. Phys.* **1969**, *51*, 2866–2870.
- (36) Lassette, E. N.; Skerbele, A.; Dillon, M. A.; Ross, K. J. *J. Chem. Phys.* **1968**, *48*, 5066–5096.
- (37) da Silva, E. C.; Gerratt, J.; Cooper, D. L.; Raimondi, M. *J. Chem. Phys.* **1994**, *101*, 3866–3887.
- (38) Nakamura, K.; Osamura, Y.; Iwata, S. *Chem. Phys.* **1989**, *136*, 67–77.
- (39) Roos, B. O.; Andersson, K.; Fülscher, M. P. *Chem. Phys. Lett.* **1992**, *192*, 5–13.